SEDIMENTARY AND TECTONIC EVOLUTION OF A TRENCH-SLOPE BASIN IN THE NANKAI SUBDUCTION ZONE OF SOUTHWEST JAPAN

MICHAEL B. UNDERWOOD,[1] GREGORY F. MOORE,[2] ASAHIKO TAIRA,[3] ADAM KLAUS,[4] MOYRA E.J. WILSON,[5] CHRISTOPHER L. FERGUSSON,[6] SATOSHI HIRANO,[7] JOAN STEURER,[1] AND THE LEG 190 SHIPBOARD SCIENTIFIC PARTY[8]

[1] *Department of Geological Sciences, University of Missouri, Columbia, Missouri 65211*
e-mail: UnderwoodM@missouri.edu

[2] *Department of Geology and Geophysics, University of Hawaii, Honolulu, Hawaii 96822*

[3] *CDEX, Japan Marine Science and Technology Center, Yokosuka, 237–0061, Japan*

[4] *Ocean Drilling Program, Texas A&M University, College Station, Texas 77845*

[5] *Department of Geological Sciences, University of Durham, Durham, DH1 4EL, U.K.*

[6] *School of Geosciences, University of Wollongong, Wollongong, NSW, 2522, Australia*

[7] *IFREE, Japan Marine Science and Technology Center, Yokosuka, 237–0061, Japan*

[8] *Keir Becker, University of Miami, Miami, FL; Luann Becker, University of Hawaii, Honolulu, Hawaii; Babette Boeckel, Universitaet Bremen, Bremen, Germany; Barry Cragg, University of Bristol, Bristol, U.K.; Allison Dean, Western Washington University, Bellingham, Washington; Pierre Henry, École Normale Supérieure, Paris, France; Toshio Hisamitsu, University of Tokyo, Tokyo, Japan; Sabine Hunze, Geowissenschaftliche Gemeinschaftsaufgaben—GGA, Hannover, Germany; Miriam Kastner, Scripps Insitution of Oceanography, La Jolla, California; Alex Maltman, University of Wales, Aberystwyth, U.K.; Julia Morgan, Rice University, Houston, Texas; Yuki Murakami, Hiroshima University, Higashi-Hiroshima, Japan; Demian Saffer, University of Wyoming, Laramie, Wyoming; Mario Sánchez-Gómez, Universidad de Jaén, Jaén, Spain; Elizabeth Screaton, University of Florida, Gainesville, Florida; David Smith, University of Rhode Island, Narragansett, Rhode Island; Arthur Spivak, University of Rhode Island, Narragansett, Rhode Island; Harold Tobin, New Mexico Institute of Mining and Technology, Socorro, New Mexico; and Kohtaro Ujiie, National Science Museum, Tokyo, Japan*

ABSTRACT: **Leg 190 of the Ocean Drilling Program yielded discoveries about the early stages of tectonic and sedimentary evolution of a trench-slope basin in the Nankai subduction zone of southwest Japan. Lithofacies character, biostratigraphy, and seismic-reflection data show that the basin's architecture was constructed during the early Quaternary by frontal offscraping of coarse-grained trench-wedge deposits. Clast types in muddy gravel beds indicate that one of the trench's polymictic sources was enriched in low-grade metasedimentary rocks. Outcrops of the Shimanto Belt on the island of Shikoku contain comparable lithologic assemblages, so we suggest that some of the turbidity currents and debris flows were funneled from that source through a transverse canyon–channel system. Offscraped trench deposits are mildly deformed and nearly flat lying beneath the slope basin. Bedding within the basin laps onto a hanging-wall anticline that formed above a major out-of-sequence thrust fault. Rapid uplift brought the substrate above the calcite compensation depth soon after the basin was created. The sediment delivery system probably was rerouted during subduction of the Kinan seamounts, thereby isolating the juvenile basin from coarse sediment influx. As a consequence, the upper 200 meters of basin fill consist of nannofossil-rich hemipelagic mud with sparse beds of volcanic ash and thin silty turbidites. Intervals of stratal disruption are also common, and the soft-sediment folding resulted from north- to northeast-directed gravitational failure. The Nankai accretionary prism has grown 40 km in width during the past 1 My, and the slope basin is already filled to its sill point on the seaward side. The stratigraphy displays an upward fining and thinning trend, in contrast to the upward coarsening and thickening mega-sequences depicted by some conceptual models for slope basins.**

INTRODUCTION

Confined turbidite basins can be found in a wide variety of tectonic settings (Prather et al. 1998; Sinclair and Tomasso 2002). Trench-slope basins form along all types of subduction margins, even those that experience non-accretion or subduction-erosion (Underwood and Moore 1995). Knowledge of sedimentary successions within such basins is based largely on interpretations of seismic reflection profiles, which typically show ponded sediments trapped behind the tectonic ridges that characterize the underlying accretionary prism (G.F. Moore and Karig 1976). We know that these environments must adjust to a dynamic interplay between tectonics and sedimentation, but our ability to document their stratigraphic and structural evolution in detail has been hampered by a lack of ground truth. Leg 190 of the Ocean Drilling Program (ODP) included the first attempt to core continuously through a modern trench-slope basin into the underlying accretionary prism. The study area is located in the central Nankai forearc, offshore Shikoku, Japan (Fig. 1). Our documentation of tectonostratigraphy within this active example permits modification of a conceptual framework that was based largely on interpretations of ancient inferred analogues.

Origin of Trench-Slope Basins

In most accretionary subduction margins (e.g., Nankai, Cascadia, Aleutians, Sunda, Makran, New Zealand, Barbados), hanging-wall anticlines form as individual thrust sheets slide over ramps (Boyer and Elliot 1982). Such anticlinal structures create linear bathymetric highs that shape the margin's structural grain (e.g., Lewis et al. 1988; Davis and Hyndman 1989; MacKay et al. 1992). Seismic reflectors within slope basins are usually tilted landward, and their dips become steeper with increasing depth in the basin because of progressive vertical movement of the marginal tectonic ridges (G.F. Moore and Karig 1976). Basins generally increase in surface area upslope as sediment buries extinct tectonic ridges, and there is a concomitant upslope increase in total sediment thickness (Karig et al. 1980; Stevens and Moore 1985). Some stratigraphic successions of this type reach 3000 m or more in thickness (Davey et al. 1986), but most slope basins contain less than 1000 m of sediment (Underwood and Moore 1995).

Slope basins change structurally through time in response to progressive subduction-driven deformation. Combinations of thrusting, folding, and diapiric intrusion modify the unconformable boundary between slope sediments and the underlying accretionary prism (G.F. Moore and Karig 1976; Scholl et al. 1980; Brown 1990). Larger basins dismember when out-of-sequence reverse, strike-slip, and/or oblique-slip faults propagate through their interiors. Subduction of seamounts also can reshape forearc structural fabrics on a regional scale and trigger large-scale mass-wasting events (Lallemand et al. 1989; Yamazaki and Okamura 1989; Dominguez et al. 2000). The net effect of these processes is to obscure a given basin's original three-dimensional lithofacies and structural architecture.

Facies Model for Trench-Slope Basins

Steeper seafloor gradients on rugged trench slopes promote bypassing of coarser sediment and/or erosion by turbidity currents. Most slope apron

JOURNAL OF SEDIMENTARY RESEARCH, VOL. 73, NO. 4, JULY, 2003, P. 589–602
 1527-1404/03/073-589/$03.00

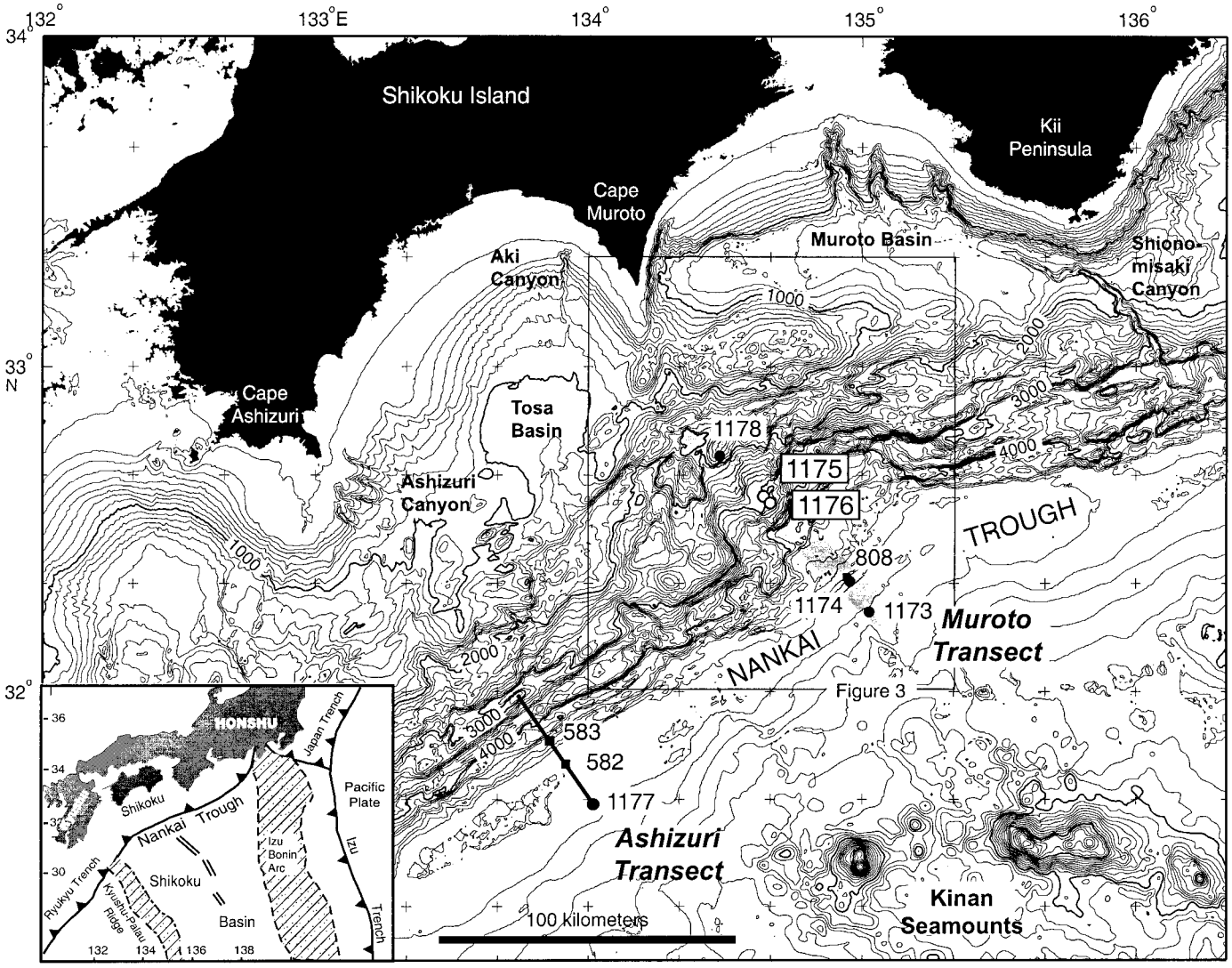

FIG. 1.—Regional bathymetric map of the Nankai Trough and the northern edge of Shikoku Basin. Numbers refer to sites of the Deep Sea Drilling Project (DSDP) and the Ocean Drilling Program (ODP). Shaded region along the Muroto Transect corresponds to area of 3-D seismic survey. Bathymetry is in meters. Modified from Shipboard Scientific Party (2001e).

deposits are fine grained because they originate via slow hemipelagic settling. Strata within trench-slope basins should be thicker and sandier than the hemipelagic slope apron because flatter seafloor gradients promote momentum decay and deposition from sediment gravity flows (Komar 1970; Middleton and Hampton 1976). In addition, large bathymetric obstructions block or deflect most downslope flow paths (Pantin and Leeder 1987; Kneller et al. 1991; Alexander and Morris 1994). During their early stages near the base of slope, direct connections from basins to the shoreline via submarine canyons or channels are rare, so the flux of terrigenous sediment tends to be relatively low. Deposits within these so-called immature slope basins consist mostly of hemipelagic mud, lutite turbidites, and locally generated slides and mudflows (Underwood and Bachman 1982). Distinctions are subtle between the immature slope-basin facies and the hemipelagic facies of the surrounding slope apron.

Accretionary prism uplift should combine with downslope canyon–channel erosion to increase flux of coarse siliciclastic sediments into slope basins through time (Underwood and Bachman 1982). Once through-going conduits are established, gravity flows bypass upslope obstructions more efficiently, thereby increasing rates of sedimentation in the basins by a factor of ten or more (G.F. Moore and Karig 1976; Underwood and Moore 1995). Consequently, stratigraphic evolution of trench-slope basins should create upward thickening and coarsening mega-sequences (Fig. 2).

Coring of modern trench-slope basin deposits has been meager (e.g., Kulm et al. 1973; Underwood and Norville 1986). The stratigraphic model (Fig. 2) is actually a conceptual collage that includes interpretations of the rock record (e.g., Moore et al. 1980; van der Lingen and Pettinga 1980; George 1992). Such interpretations are seldom straightforward, however, and alternative views have been expressed even for the ''type example'' of Nias Island (e.g., Samuel and Harbury 1996). One dilemma is that lithofacies criteria cannot be used to discriminate definitively between accreted trench-wedge and slope-basin deposits (Underwood and Bachman 1982). Another consideration in such studies is the style of deformation (Smith et al. 1979; Moore and Karig 1980; Moore and Allwardt 1980; Bachman 1982; Hibbard et al. 1992). Inferred slope-basin deposits typically display tight asymmetric folds, mesoscale thrust faults, and evidence of increasing shear towards contacts with more highly deformed melange units interpreted to be an accretionary prism. The contrast in stratal disruption is not a reliable criterion either, because strain partitioning can occur for a variety

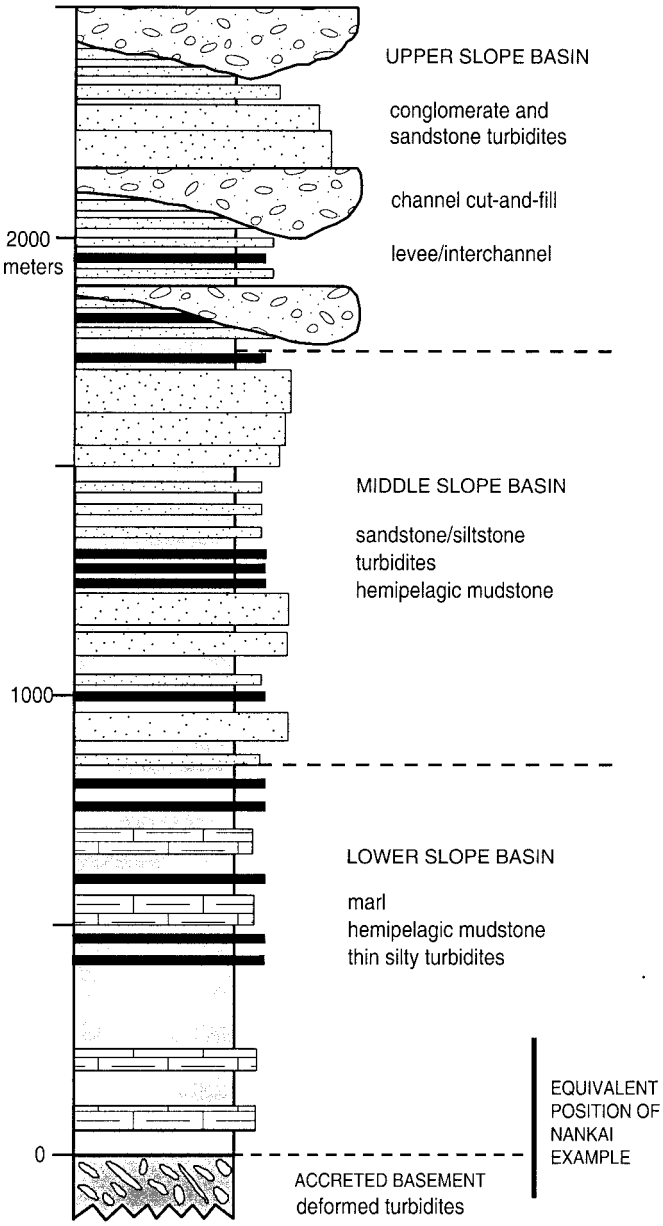

FIG. 2.—Hypothetical model for stratigraphic evolution of a trench-slope basin, based largely on the observations of Moore et al. (1980) on Nias Island, Indonesia. The upward coarsening and thickening megacycle is the result of basin uplift and temporal increases in terrigenous influx. Smaller-scale cycles are due to progradation or lateral migration of depositional lobes (upward thickening) and migration or abandonment of channels (upward fining and thinning). Modified from Underwood and Moore (1995).

of reasons within deeper levels of a subduction complex. If, for example, abyssal-plain turbidites enter a subduction zone and underplate by duplexing, internal deformation in the domain between the roof and floor thrusts will be minimal (e.g., Sample and Moore 1987). Facies character of underplated turbidites, therefore, can be confused with the facies in slope-basin successions (Underwood and Laughland 2001). Perhaps the most convincing evidence for slope-basin deposition is an assemblage of fossils that indicate intermediate water depths, progressive uplift, and shoaling (e.g., Moore et al. 1980), but such information is not commonly available.

Leg 190 of the Ocean Drilling Program (ODP) provided us with an opportunity to document the early stages of stratigraphic evolution of a trench-slope basin within the Nankai subduction system of southwest Japan (Fig. 1). We drilled and cored continuously through the basin–prism contact at two sites seaward of the Muroto Peninsula of Shikoku (Holes 1175A and 1176A). Drilling data from the Muroto study area complement seismic profiles from a 3-D reflection survey, detailed bathymetry, and side-scan sonar (Moore et al. 2001). These data add new complexities to our theories regarding subduction-margin sedimentation.

NANKAI TROUGH

Several deep-sea trenches border the Japanese island arc system (Fig. 1). Plate convergence in the Nankai Trough is slightly oblique; youthful oceanic lithosphere of the Shikoku Basin (Philippine Sea Plate) is subducting at a rate of 2–4 cm/yr (Karig and Angevine 1986; Seno et al. 1993). Rifting of the proto-Izu–Bonin arc and back-arc spreading created the subducting plate (Taylor 1992). Rifting began during the Oligocene, and seafloor spreading in the back-arc basin lasted until ~ 15–12 Ma (Chamot-Rooke et al. 1987; Okino et al. 1994). The Kinan seamount chain (Fig. 1) sits above the extinct spreading axis (Le Pichon et al. 1987a). Sedimentary deposits throughout the upper part of the Shikoku Basin consist of hemipelagic mudstone and volcanic ash (Pickering et al. 1993). The lower part of the basin, however, changes its facies character considerably along strike. Above basement highs associated with the Kinan seamounts, the lower Pliocene and Miocene strata consist predominantly of hemipelagic mudstone and altered vitric mudstone (Taira et al. 1992; Shipboard Scientific Party 2001a). Above basement plains (e.g., along the Ashizuri transect), the lower Shikoku Basin facies includes abundant siliciclastic turbidites (Shipboard Scientific Party 1975; Pickering et al. 1993; Shipboard Scientific Party 2001b).

Water depth along the axis of the Nankai Trough is less than 5,000 m, and the axial gradient dips gently to the southwest (Fig. 1). Rates of sediment delivery to the trench are high because of rapid uplift and erosion within the main detrital source area: the collision zone between the Honshu Arc and the Izu–Bonin Arc (Taira and Niitsuma 1986; Soh et al. 1991; Marsaglia et al. 1992; Underwood et al. 1993). The largest through-going sediment conduit is Suruga Trough; this submarine canyon extends from the shoreline on the west side of the Izu Peninsula and continues along the northern flank of Zenisu Ridge into the northeast end of the Nankai Trough (Le Pichon et al. 1987b; Nakamura et al. 1987; Soh et al. 1995). The Nankai deep-sea channel extends from its inception point in Suruga Trough down the axis of Nankai Trough to a termination point offshore from the Kii Peninsula (Shimamura 1989). Fan-shaped sediment mounds occur at the mouths of Tenryu and Shiono-misaki canyons (Soh et al. 1991), and several smaller canyons probably reach the trench (Taira and Ashi 1993). Seismic-reflection records and drilling show that the trench wedge is typically 450 to 700 m thick, and the facies thicken and coarsen upward (J.C. Moore and Karig 1976; Coulbourn 1986; Taira et al. 1992).

The geologic record of subduction-accretion includes onland Cretaceous–Miocene exposures of the Shimanto Belt (Taira et al. 1988). The present-day Nankai accretionary prism began to form approximately 8–6 Ma (Taira et al. 1992). Thrust faults and folds have created a forearc with rugged ridge-and-trough landscape (Le Pichon et al. 1987a, 1987b; Moore et al. 1991; Ashi and Taira 1992; Morgan et al. 1994; Okino and Kato 1995). Several prominent basins on the upper slope (e.g., Muroto and Tosa basins) intercept sediment transport from small canyons and slope gullies (Blum and Okamura 1992). A conspicuous indentation of the structural grain near the Muroto Peninsula (Fig. 3) probably was caused by subduction of seamounts associated with the Kinan chain (Yamazaki and Okamura 1989; Park et al. 1999; Kodaira et al. 2000).

Geological Context of Leg 190 Sites

Structural architecture of the Nankai accretionary prism varies markedly along strike (e.g., Ashi and Taira 1992; Morgan et al. 1994). Bathymetry

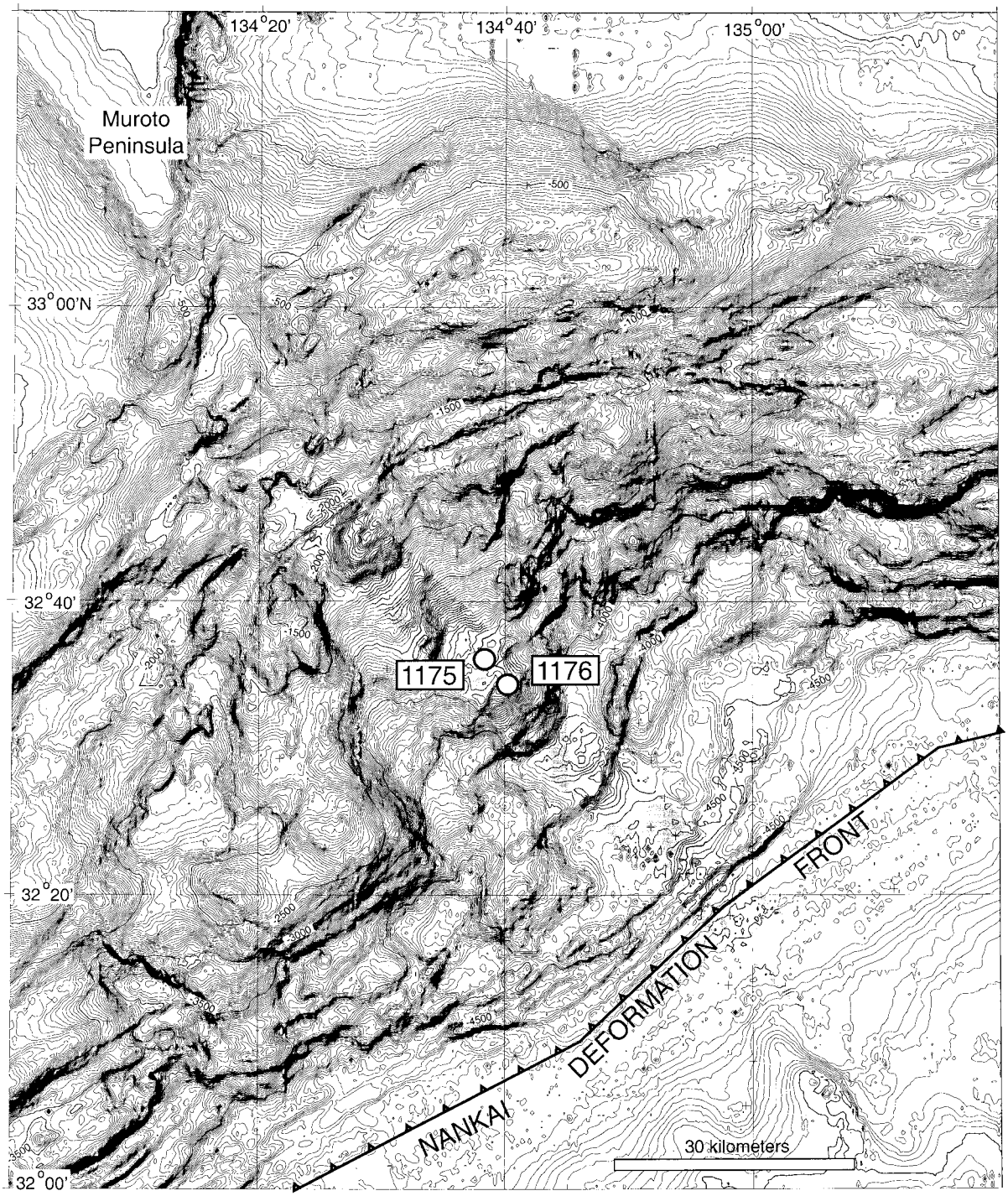

FIG. 3.—Detailed bathymetric map of the Nankai forearc within the Muroto Transect area. See Figure 1 for regional context. Contour interval is 20 m. Numbers refer to ODP drill sites. Shaded region corresponds to area of 3-D seismic survey. Modified from Moore et al. (2000).

is rugged, with irregular ridges and steep scarps (Fig. 3). The Muroto segment (Fig. 1) includes ODP Sites 1175 and 1176. Moore et al. (2001) subdivided the Muroto segment into four structural divisions (Fig. 4). Starting at the prism toe, the imbricate-thrust zone is characterized by packages of seaward-vergent thrust faults, with the frontal thrust forming its seaward edge. A system of out-of-sequence thrusts begins about 20 km landward of the deformation front. These faults displace older structures that are equivalent to those within the imbricate-thrust zone. The lowermost slope basin within the Muroto transect is located behind a ridge that was created by uplift along the frontal out-of-sequence thrust (Fig. 4). The third structural subdivision is called the large-thrust-slice zone, where at least four distinctive faults separate previously imbricated packages of relatively coherent sedimentary strata. Underplating of Shikoku Basin strata may be the cause of strong reflectors beneath the large thrust slices. Slope sediments above the faults are tilted landward, indicating recent uplift. ODP Hole 1175A penetrated a second slope basin just landward of a major out-of-

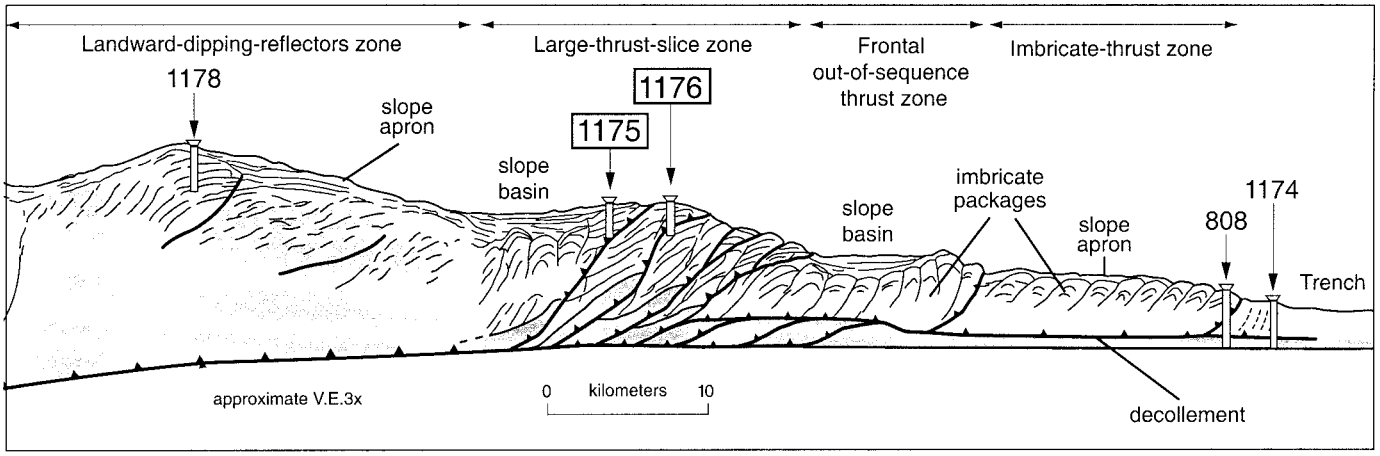

FIG. 4.—Interpretive cross section of the Nankai accretionary prism showing four zones of seismic-reflection structure within the Muroto Transect area (modified from Shipboard Scientific Party 2001e). Numbers refer to ODP drill sites. See Figure 3 for location of 3-D seismic survey, which includes the plane of the cross section.

sequence thrust (Fig. 4), at a water depth of 3012.8 m below sea level. ODP Hole 1176A drilled through a separate fault slice at the seaward edge of the same basin, at a depth of 3016.8 m below sea level. Farther up slope, the fourth structural zone displays semicontinuous landward-dipping reflectors beneath a relatively coherent apron of slope sediments.

DRILLING RESULTS

ODP Hole 1175A was cored by APC (advanced hydraulic piston corer) from the mudline to 205.3 mbsf (meters below seafloor) with 99% recovery. The extended core barrel (XCB) system was then deployed from 205.3 to 445.5 mbsf with 54% recovery. At Site 1176, the APC was used to a depth of 170.6 mbsf with 92% recovery, and the XCB penetrated from 170.6 to 449.6 mbsf with 27% recovery. Nannofossils from the cores show that the age of the underlying Nankai accretionary prism is young (< 4 Ma) within our region of interest (Fig. 5). We subdivided the strata into three lithostratigraphic units: upper slope-basin (unit I), lower slope-basin (unit II), and slope-to-prism transition (unit III). We then attempted to match the facies changes with acoustic character and physical properties. Overall, the stratigraphic succession decreases in grain size and bed thickness up section (Fig. 5). The following summary is meant to highlight the salient details of our shipboard descriptions and measurements (Shipboard Scientific Party 2001c, 2001d).

Lithostratigraphy

Upper Slope-Basin Facies.—Unit I is Quaternary in age and extends from the seafloor to depths of 224.75 mbsf (Site 1175) and 195.79 mbsf (Site 1176). Hemipelagic mud is the most common lithology within this upper slope-basin facies (Fig. 6). The silty clay is enriched in calcareous nannofossils. Internal structure of the mud is homogeneous to faintly laminated or mottled due to bioturbation. Calcite content within the mud deposits is due largely to nannofossils. Relative percentages of calcite average 23 and 25%. Strata at Site 1175 show a clear increase in carbonate down section, but the pattern at Site 1176 is more complicated (Fig. 7). Local beds of volcanic ash vary in thickness from less than a centimeter to over two meters. The ash layers typically have sharp, plane-parallel to irregular lower contacts and gradational upper contacts. One unusually thick ash bed occurs at a depth of 92.7–95.0 mbsf in Hole 1175A. Sand, clayey sand, and silt occur locally as laminae and thin beds with sharp bases, diffuse tops, and normal grading (Fig. 6). Most such deposits probably resulted from fine-grained turbidity currents. Contorted stratification is the most noteworthy aspect of unit I, particularly at Site 1175. Common manifestations of soft-sediment deformation include steeply inclined layers of silt and volcanic ash and small-scale recumbent to inclined folds. Some intervals contain curviplanar to irregular fragments of nannofossil-rich mud and ash engulfed in a matrix of mud.

Lower Slope-Basin Facies.—Unit II is also Quaternary in age and extends from 224.75 to 301.64 mbsf at Site 1175 and from 195.79 to 223.54 mbsf at Site 1176 (Fig. 5). Lithification is more advanced than in unit I, and soft-sediment deformation is absent. The distinguishing lithology of the lower slope-basin facies is poorly sorted and structureless sandy mudstone, whose uppermost occurrence defines the top of unit II. Other lithologies include hemipelagic mudstone, as well as thin beds and laminae of volcanic ash and fine sand (Fig. 6). Total carbonate content (from X-ray diffraction) and nannofossil abundance (from smear slides) are generally comparable to values from the bottom of unit I (Fig. 7).

Slope Basin-to-Prism Transition.—The most characteristic aspect of unit III, which is Quaternary to Pliocene in age, is its abundance of poorly indurated, thin- to medium-bedded silt and sand turbidites (Fig. 5). Typical internal sedimentary structures include normal size grading, plane-parallel laminae, and ripple cross-laminae (Fig. 6). Grain size varies from very coarse sand to silt. Lower surfaces are sharp and planar to scoured; upper contacts are diffuse and gradational. All of these features are consistent with transport and deposition by turbidity currents. The most exceptional lithology within unit III is muddy gravel to pebbly mud (Fig. 6). The pebbly mud is poorly sorted throughout. Its clast fabric is disorganized; internal stratification is absent, and clasts are supported partially to completely by a muddy matrix. The matrix is composed of silty clay, similar in composition to the interbeds of hemipelagic mudstone. Clasts are rounded to subrounded and are up to 5.5 cm in diameter. A polymictic population of clasts includes abundant quartz, chert, fine-grained sedimentary to metasedimentary lithic fragments, and minor fragments of mafic volcanic rock. Beds of hemipelagic mudstone and/or sandy mudstone typically occur between the coarse-grained sand and gravel beds. Relative abundance of calcite (largely in the form of micrite cement) decreases sharply within the mudstones of unit III; the average value for unit III is 10% at Site 1175 and 3% at Site 1176 (Fig. 7).

Biostratigraphy

Calcareous nannofossils provide a continuous record of Pliocene to Holocene deposition, and several datums allow us to correlate between the two slope-basin sites (Fig. 5). The Pliocene–Pleistocene boundary (1.8 Ma) is located at a depth of 389.27 mbsf in Hole 1175A and at 291.63 mbsf in Hole 1176A (Fig. 5). The top of zone NN18 (1.95 Ma) occurs at depths

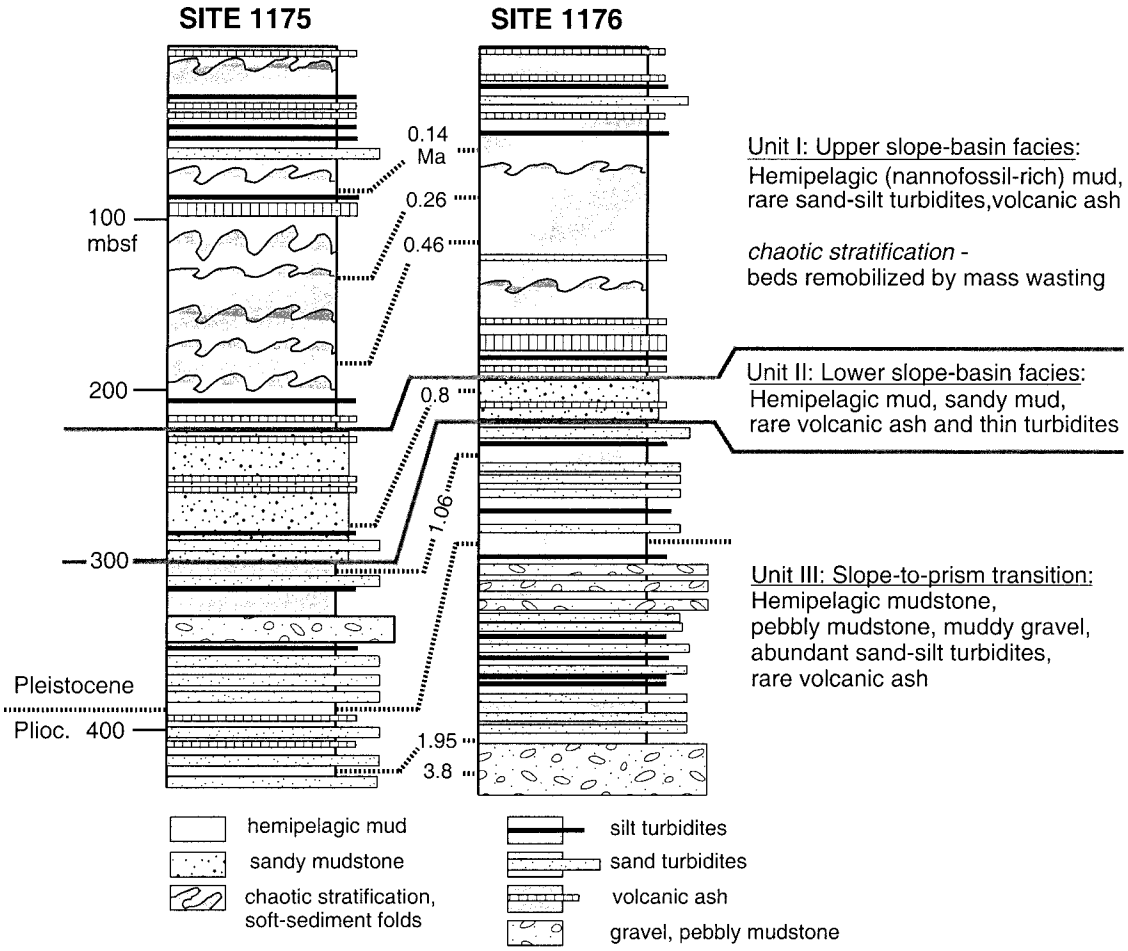

FIG. 5.—Lithostratigraphic and biostratigraphic correlation for Sites 1175 and 1176 of the Ocean Drilling Program, Nankai forearc. Stratigraphic ages (Ma) are based on nannofossil zones (Shipboard Scientific Party 2001c, 2001d).

of 416.77 mbsf (Hole 1175A) and 407.20 mbsf (Hole 1176A). Fossils from Site 1176 extend to Zone NN15 (3.8 Ma), but the abundance and preservation of nannofossils deteriorate markedly within unit III. Calculated rates of sedimentation (uncorrected for compaction) are highly variable (113 to 2859 m/My) within the slope-basin facies (units I and II), although we note that stratal disruption (described below) distorts the primary depositional thickness within the upper 200 meters. Rates of sedimentation within unit III ranged from 10 to 770 m/My.

Structural Geology and Physical Properties

The upper 205 m of Hole 1175A (unit I) are characterized by eight discrete zones of core-scale recumbent to isoclinal folds, chaotic mixing of lithologies, and fragmentation of bedding. Between these zones, which range from 3 to 10 m in thickness, are intervals with horizontal to gently inclined beds. Stratal disruption is comparatively subtle in Hole 1176A, where only two discrete zones were recognized. Fold amplitudes vary from a few centimeters to several meters (inferred from down-core changes in bedding attitudes). Some of the stratal disruption observed in split core could be an artifact of (or accentuated by) the APC coring process, but exposures of tight fold hinges with sharp and undistorted intersections at the core margin indicate that most such folds formed through geologic processes. Even after using natural remanent magnetism (NRM) declination to reorient the individual pieces of core (following Shipboard Scientific Party 1991b), we found bedding attitudes to be too scattered to define a systematic trend of dip directions. Axial planes strike west–east to northwest–southeast and dip to the south and southwest; fold axes trend to the southwest with gentle to moderate plunges.

Sediment compaction profiles within the slope-basin successions are complicated because of changes in lithology and stratal disruption. Porosity values from laboratory measurements of split-core samples are highly variable within unit I (Fig. 8). Values in Hole 1175A decrease slightly with depth from 65–70% at mudline to 61–68% at ~ 100 mbsf. Porosity decreases abruptly at ~ 100 mbsf to 57–61% and then decreases gradually to ~ 200 mbsf. Porosity data from Site 1176 decrease from 70–73% at mudline to 55–60% at 200 mbsf. There is also an abrupt shift to lower porosities at approximately 60 mbsf (Fig. 8).

Most of the cores from units II and III exhibit an unexpectedly small number of mesoscale deformation features. Bedding in Hole 1175A is subhorizontal from 205 to 445 mbsf, with minor faults and a few localized zones of disruption. At Site 1176, an interval of high-angle fracturing crosses the boundary between units II and III, but bedding within unit III is likewise subhorizontal. Units II and III display a uniform compaction gradient at Site 1175, with porosity reaching values of less than 45% by 400 mbsf (Fig. 8). At Site 1176, in contrast, there is a notable decrease in porosity from 53–57% to 48–54% across the unit II–III boundary. Below 350 mbsf, values remain nearly unchanged (40–47%) to the bottom of the hole.

Seismic Stratigraphy

Site 1175.—Seismic reflection units near Site 1175 match reasonably well with the core-based lithostratigraphy (Fig. 9), in spite of the fact that

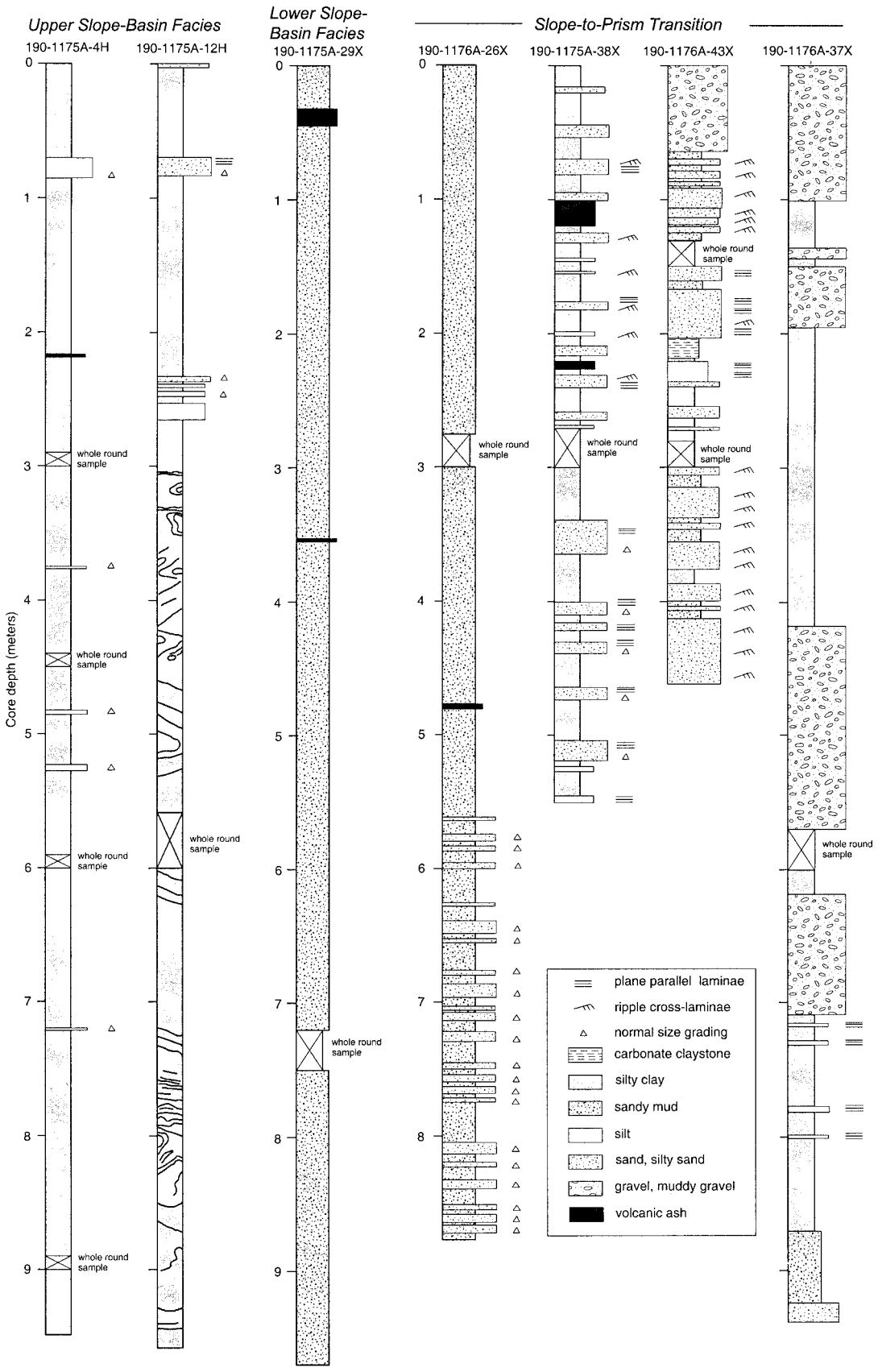

FIG. 6.—Examples of lithofacies at the scale of individual cores from ODP Holes 1175A and 1176A, Nankai forearc.

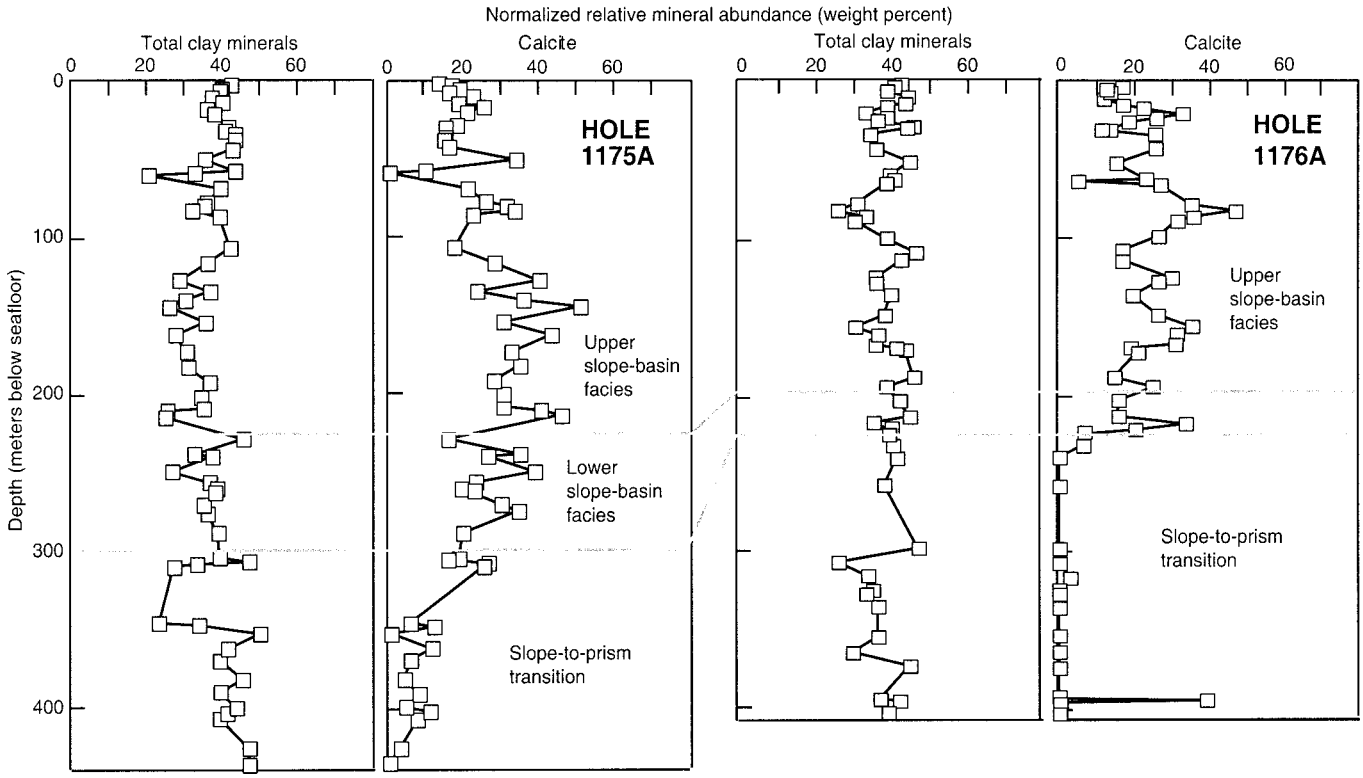

FIG. 7.—Relative abundance of calcite and total clay minerals in samples from ODP Holes 1175A and 1176A, Nankai forearc. Mineral abundance is based on X-ray diffraction analysis of random bulk powders (Shipboard Scientific Party 2001c, 2001d).

the velocity structure is not well known. Lithostratigraphic unit I coincides with seismic unit A; this seismic interval is bounded at the top by the seafloor reflector and at the bottom by an angular discordance. Reflectors are horizontal near the seafloor and steepen to 8–10° at the base of unit A. The upper 40 m of the depth section display a somewhat irregular and discontinuous reflection character, but there is little evidence for the type of widespread stratal disruption that we observed in the cores. A thick ash bed (> 232 cm at core depth 92.7–95.0 mbsf) may be the cause of a northwest-dipping high-amplitude positive reflection at approximately 110 mbsf seismic depth. If this interpretation is correct, then the velocity–depth model needs to be adjusted by at least 15 m to match the lithostratigraphy with acoustic facies.

The upper boundary of seismic unit B (equivalent to lithostratigraphic unit II) occurs at a seismic depth of approximately 250 mbsf (Fig. 9). Reflectors within the upper part of unit B are conformable with the boundary. The upper unit boundary dips gently toward the northwest, and downlap at the base of unit A creates an angular discordance. The base of acoustic unit B, in contrast, displays onlap toward the southeast. Thus, unit B is a northwest-thickening wedge with relatively continuous and high-amplitude internal reflections. The thickness of unit B is roughly 75 m in the vicinity of Site 1175 (Fig. 9), close to the core thickness of unit II (76.89 m). Core depth for the unit boundary is 224.75 mbsf, on the basis of the first occurrence of sandy mudstone. That change in lithology, however, is not likely to generate a prominent seismic reflection, and there is no systematic shift in porosity across the lithofacies boundary to account for the contrast in acoustic impedance (Fig. 8).

Seismic unit C correlates with lithostratigraphic unit III. The upper part of unit C is subparallel to the unit boundary, but its base is ill defined (Fig. 9). The core depth of the unit II–III boundary is 301 mbsf, whereas the seismic depth to the unit B–C boundary is approximately 325 mbsf. Shipboard measurements show a decrease in porosity below 325 mbsf (Fig. 8), and this shift may be a consequence of tectonic consolidation rather than a facies change. We interpret the prominent reflectors below the unit B–C seismic boundary as thick beds of gravel and pebbly mud that begin at core depth 340 mbsf. Reflectors within unit C become increasingly irregular and discontinuous below a seismic depth of 400 mbsf (Fig. 9).

Site 1176.—Reflection packages near Site 1176 correlate more closely with lithostratigraphic boundaries than at Site 1175 (Figs. 8 and 10). Reflections within the upper 80 m of unit A are generally continuous and dip gently to the southeast (seaward); reflections below a seismic depth of 80 mbsf are discontinuous and dip gently landward. Acoustic unit A is wedge shaped, bounded at the top by the seafloor and at the bottom by a strong continuous reflector that dips gently to the northwest. The acoustic boundary intersects Hole 1176A at about 180 mbsf, whereas the core depth for the unit I–II boundary is 195.79 mbsf, on the basis of the first occurrence of sandy mudstone. As at Site 1175, that lithologic change is not likely to cause a pronounced impedance contrast, so we suspect that the prominent reflector at 180 mbsf seismic depth is related to a partially recovered ash layer in core 20X (drilled 170.6–180.2 mbsf).

Acoustic unit B correlates crudely with lithostratigraphic unit II. Its lower boundary is highly irregular and appears as a broad antiformal surface with a seismic depth of approximately 230 mbsf near Site 1176. To the northwest of Site 1176, strong and continuous reflectors within acoustic unit B lap onto this irregular surface and thicken landward (Fig. 10). Reflectors are discontinuous and decrease in amplitude southeast of Site 1176.

The transition into acoustic unit C (~ 230 mbsf) is probably related to an abrupt shift in porosity near the unit II–III boundary (core depth 223.54 mbsf). To the northwest of Site 1176, internal reflections within unit C are high in amplitude, laterally continuous, and dip to increasingly steep angles toward land. Reflectors are nearly flat lying near Site 1176, and some roll over to the southeast, thereby defining an antiformal geometry. This large structure is a fault-bend fold in the hanging wall of an out-of-sequence

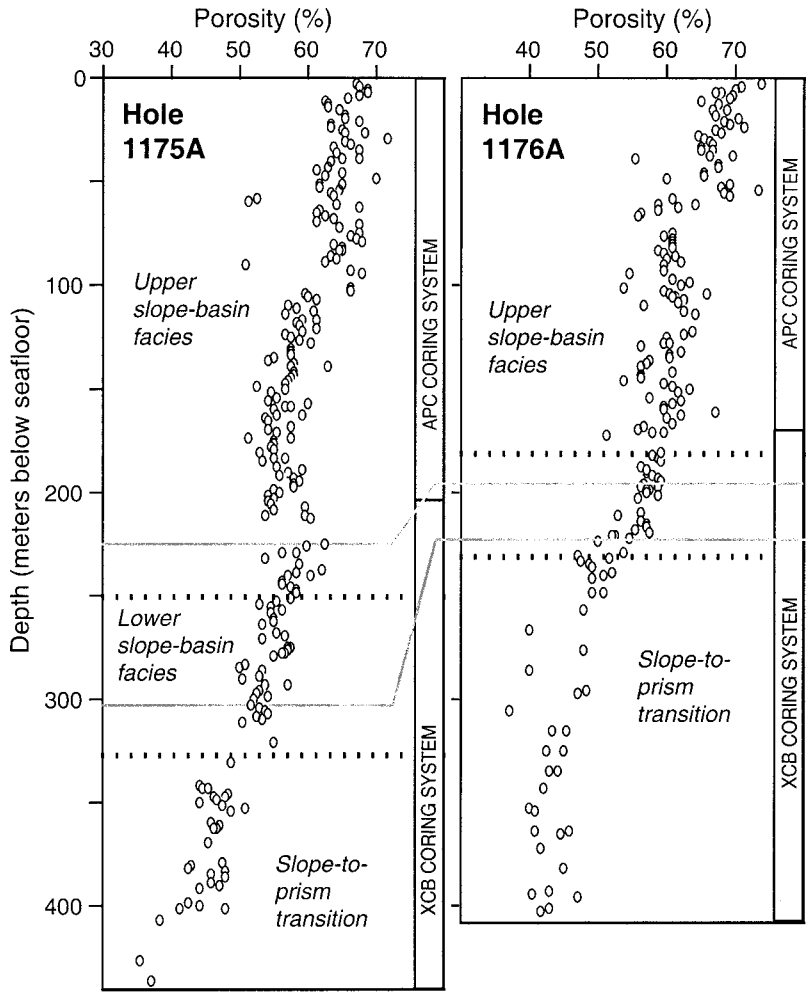

FIG. 8.—Variations in porosity with depth in ODP Holes 1175A and 1176A, Nankai forearc (Shipboard Scientific Party 2001c, 2001d). Solid lines denote boundaries between lithostratigraphic units (see Fig. 5). Dotted lines denote boundaries between seismic-stratigraphic units (see Figs. 9 and 10). Also shown are depth ranges for APC (advanced hydraulic piston corer) and XCB (extended core barrel) coring systems.

thrust that lies approximately 10–20 m below the base of Hole 1176A (Fig. 10).

DISCUSSION

Interpretation of Basin–Prism Boundary

Based on assessments of seismic-reflection and coring data, we place the contact between the Nankai accretionary prism and overlying slope-basin deposits within a few meters of the core-scale boundary between lithostratigraphic units II and III. Pinpointing the location of the boundary is problematic. Core depth and seismic depth of this boundary are within 10 m of one another at Site 1176, but the mismatch is closer to 25 m at Site 1175. In addition to possible errors in the velocity model, the mismatch is rooted in our interpretation of two overlapping sets of physical variables. Decreases in porosity within lithologic unit III (Fig. 8) are consistent with higher amounts of tectonic consolidation within the accretionary prism. Abrupt shifts in physical properties at core depths of ~ 325 mbsf and ~ 225 mbsf are probably responsible for the impedance contrast between acoustic units B and C. On the other hand, the changes in grain size and bed thickness toward and across the facies boundary are more gradual (Fig. 5). The only sharp change that we noted in composition occurs in calcite content, which increases substantially above ~ 310 mbsf in Hole 1175A and above ~ 223 mbsf in Hole 1176A (Fig. 7). This increase in carbonate was probably caused by calcareous nannofossils diluting the supply of suspended terrigenous silt and clay. The depositional substrate, which is currently ~ 3015 m below sea level, evidently rose above the calcite compensation depth during the early stages of uplift of the frontal accretionary prism.

Another criterion to consider in evaluating the basin-to-prism boundary is structural style. In theory, slope-apron and slope-basin deposits should be less deformed than rocks of the underlying accretionary basement (Smith et al. 1979; Moore and Karig 1980; Moore and Allwardt 1980; Bachman 1982; Hibbard et al. 1992). In the Nankai example, however, not only are the accreted strata essentially undeformed at core scale, their bedding planes are horizontal to subhorizontal. Our explanation for this unexpected discovery is the development of a hanging-wall anticline near Site 1176 (Fig. 10). The out-of-sequence thrust fault beneath the anticline displays a ramp-to-flat transition immediately beneath Site 1176 (Fig. 10). A similar structure controls bedding orientation within unit III near Site 1175 (Figs. 4 and 9).

Sedimentologic criteria are, likewise, inconclusive as a means of separating uplifted trench-wedge strata from coarse-grained slope-basin deposits. The tectono-stratigraphic environment for the upper part of unit III remains somewhat ambiguous, so we offer two possible interpretations for the gradual change in sedimentary facies across the structural transition. The modern Nankai trench wedge receives its turbidite input from a combination of axial and transverse flow paths (Taira and Niitsuma 1986; Soh et al. 1991; Pickering et al. 1992; Underwood et al. 1993; Taira and Ashi 1993). Some of the thin sand beds within the upper part of unit III may have been deposited on the frontal ridge when thicker turbidity currents moved across the trench floor and lapped onto the landward wall. Supporting evidence for this suggestion comes from the uppermost lithostrat-

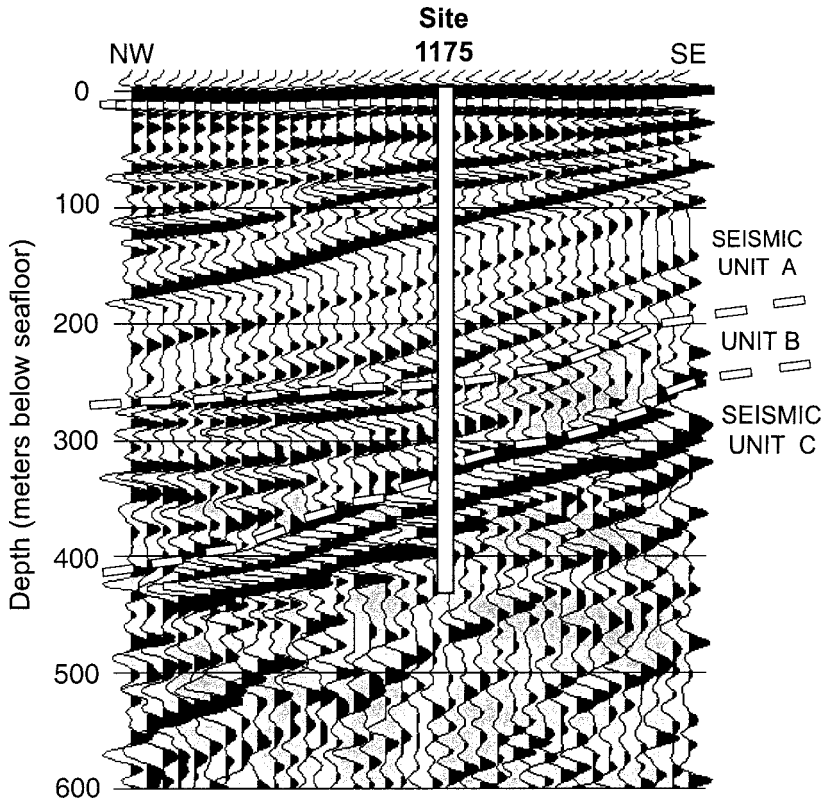

FIG. 9.—Segment of seismic reflection profile through ODP Site 1175, Nankai forearc (modified from Shipboard Scientific Party 2001c). Depth scale (m below seafloor) is based on a first-iteration velocity model. Horizontal distance is approximately 1.8 km. See Figure 8 for comparison between seismic units and lithostratigraphic units.

igraphic unit at ODP Site 808 (Fig. 1), which consists of approximately 20 m of thin-bedded turbidites that were deposited 150 m above the trench floor (Shipboard Scientific Party 1991a; Taira et al. 1992).

A preponderance of coarse-grained deposits within unit III favors a scenario in which subdued seafloor gradients promoted rapid deceleration and deposition of frequent debris flows and turbidity currents. The flat floor of the Nankai Trough satisfies this expectation better than a steeply inclined frontal ridge. Forearc bypassing can occur in the form of unconfined turbidity currents (Underwood 1991), but submarine canyons are the most efficient agents for delivery of coarse sediment to trench-wedge environments (Underwood and Karig 1980; Taira and Ashi 1993). The second interpretation to consider, therefore, is frontal accretion of trench-wedge deposits close to the mouth of a submarine canyon. Perhaps a canyon maintained its flow path by eroding across a newly formed slope basin during the initial uplift of the frontal ridge. If so, then the juvenile basin would have continued to receive a substantial amount of transverse turbidite input during its early history, thereby blurring the facies distinction between trench and slope basin.

Stratigraphic Evolution of Slope Basin

One of the more significant discoveries during Leg 190 is the age of accreted basement beneath Sites 1175 and 1176. If our interpretations regarding the unit II–III contact relations and facies changes are correct, then the youngest accreted turbidites are only about 1 Ma (Fig. 5). This time constraint means that a 40-km-wide swath of accretionary prism was added to the Nankai margin over that same 1 My time period. Even if the actual slope-to-prism contact is deeper within unit III (and somewhat older), the rate of tectonic accretion remains impressive. In comparison, the turbidite-rich Middle America accretionary prism off the coast of Mexico has grown approximately 23 km in width during the past 10 My (Moore et al. 1982). Uplift and denudation of the collision zone between Honshu and the Izu–Bonin Arc (Niitsuma 1989; Soh et al. 1991) probably led to increased rates of sediment delivery to the Nankai trench wedge. Such large increases in the rate of sediment supply would increase the trench-wedge width and the rate of frontal accretion (Mountney and Westbrook 1996).

The clast population of muddy gravel deposits within lithostratigraphic unit III indicates that their detrital source was enriched in low-grade metasedimentary rocks. Correlative rocks crop out in the Shimanto Belt of southwest Japan (Taira et al. 1988). Rigorous petrographic analysis of the ODP sand layers will be needed to establish their provenance, but the island of Shikoku is a logical source. As discussed above, the depositional environment for unit III may have been adjacent to a through-going shelf-to-trench sediment conduit, perhaps a submarine canyon–fan system, operating in concert with the axial flow system. No such conduit exists at the present time within the Muroto transect area (Fig. 3). The closest example in the present-day physiography of the Nankai Trough is Shiono-misaki Canyon, whose head begins offshore the Kii Peninsula (Fig. 1). Aki Canyon, located $\sim$ 10 km west of the Leg 190 transect, terminates in the Tosa forearc basin (Kagami and Mitusio 1988; Blum and Okamura 1992).

Because the overall stratigraphic succession at Sites 1175 and 1176 thins and fines upward (Fig. 5), we suggest that the basin's transverse sediment delivery system must have been rerouted at about 1 Ma during the early stages of uplift, folding, and faulting of the underlying accretionary prism. Rerouting or blockage of the canyon system may have been a byproduct of forearc deformation that was caused by subduction of seamounts associated with the Kinan chain (Yamazaki and Okamura 1989; Park et al. 1999; Kodaira et al. 2000). Such reorganization of the bathymetric architecture probably intensified sediment trapping farther upslope in the Tosa and Muroto forerac basins (Blum and Okamura 1992; Taira and Ashi 1993). Once the input of sandy siliciclastic sediment to the lower slope basin was terminated, sedimentation there shifted to hemipelagic settling of nannofossil-rich mud. Hemipelagic sedimentation was interrupted occasionally by airfalls of volcanic ash and fine-grained turbidity currents that either escaped the confinement of nearby canyons (by flow stripping)

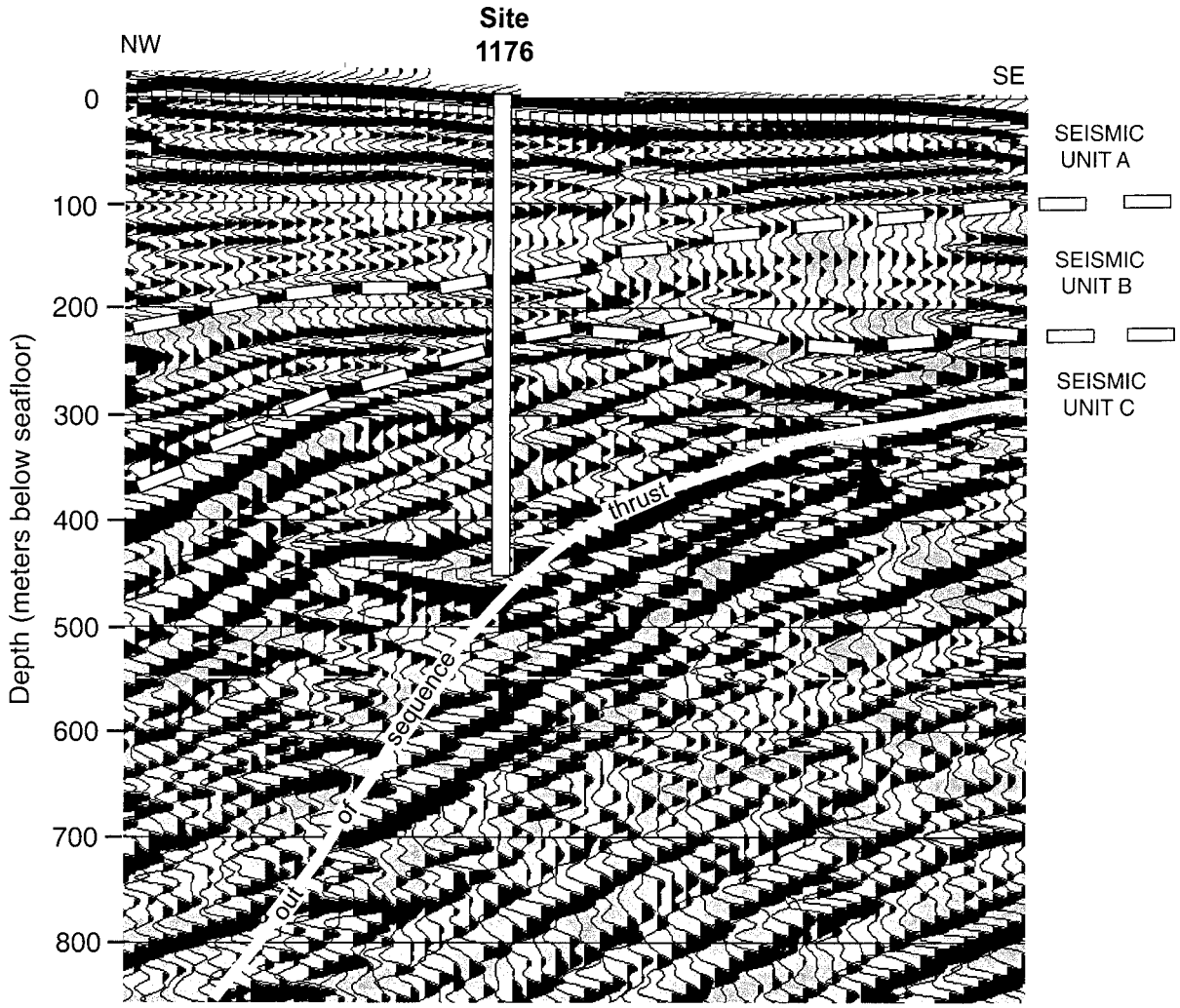

FIG. 10.—Segment of seismic reflection profile through ODP Site 1176, Nankai forearc (modified from Shipboard Scientific Party 2001d). Depth scale (m below seafloor) is based on a first-iteration velocity model. Horizontal distance is approximately 3.1 km. See Figure 8 for comparison between seismic units and lithostratigraphic units.

or flowed over or around surrounding bathymetric obstructions (e.g., Muck and Underwood 1990; Underwood 1991; Alexander and Morris 1994). Distinctive sandy mud layers in unit II probably originated as relatively fine-grained debris flows or mudflows, with the sand-size clasts fully supported by the muddy matrix. Transport could have occurred within transient channels or as unconfined flows. The higher concentration of calcareous nannofossils in the hemipelagic mud of units I and II supports the idea of uplift and deposition on a basin substrate that was elevated above the calcite compensation depth. Deposition of mud continued until the basin was filled to its seaward sill point.

The overall pattern of facies change within the Nankai slope basin (Fig. 5) matches part, but not all, of a conceptual model that is based largely on the rock exposures of Nias Island (Fig. 2). One important point to consider during such comparisons is the tendency of confined turbidite basins to evolve through several discrete stages. Some such basins, for example, pass though successive phases of structural birth, flow ponding, flow stripping, flow bypass (due either to channel incision or abandonment), and blanketing or backfilling (Prather et al. 1998; Sinclair and Tomasso 2002). This so-called ''fill-and-spill'' behavior can lead to upward thinning and fining trends during the abandonment phase. We also stress, however, that the record of sedimentation documented at Sites 1175 and 1176 spans a relatively brief timeframe of 1 My or less. The basin is still in its adolescent stage of development, with 300 m or less of total sediment accumulation. The current water depth of the basin floor is approximately 3000 m. In comparison, the Nias Beds exceed 3000 m in total thickness, and the upper turbidites are overlain unconformably by a coral reef cap (Moore et al. 1980). As we project several million years into the future, the Nankai slope basin will shoal in response to continued underplating. Downslope erosion of transverse channels should increase the influx of coarse-grained turbidites, as shown by Blum and Okamura (1992) for the present-day upper trench slope. Thus, the full evolutionary cycle of the basin could still result in the predicted upward-coarsening mega-trend.

Stratal Disruption within Upper Slope-Basin Facies

The relatively thin intervals of chaotic stratification within unit I evidently were created by local remobilization of hemipelagic sediment as the slope basin filled to capacity. According to one classification scheme for mass movements (Martinsen 1994), the types of core-scale features that we encountered span a continuum from slump (coherent mass with considerable internal deformation) to debris flow (remolded mass with plastic behavior). According to other widely used classifications, however, the term ''slump'' connotes rotation of bedding above a curved failure surface as opposed to a translational slide above a planar surface (e.g., Prior and

Coleman 1984). There is little evidence of internal deformation at the scale depicted by seismic-reflection profiles, and no hint of block rotation above discrete failure surfaces (Figs. 9, 10). Thus, the exact forms of slope failure remain ambiguous.

Remobilization of muddy slope deposits is a common phenomenon within subduction zones. The severity of slope failure ranges from sluggish downslope creep of hemipelagic mud (Baltuck et al. 1985) to prodigious slumps and slides that are capable of generating tsunamis (von Huene et al. 1989). Material recycling will occur if the failure surface excavates deep beneath the slope apron (Moore et al. 1976; Jacobi 1984; Ballance 1991). Slope failure is particularly common along the frontal ridge on the lower slope, where associated debris lobes typically extend onto the trench floor (e.g., Davis and Hyndman 1989; Ashi and Taira 1992). Likely triggering mechanisms for intraformational mass wasting include dynamic loading by seismic waves, the intrinsic weakness of porous mud on steep slopes, and oversteepening of bedding planes during episodes of uplift (Hampton et al. 1996).

We suggest that the products of mass wasting within unit I are a response to episodic back-tilting of the slope basin. Site 1175 was subjected to at least eight failure events over a time span of approximately 0.5 My. Site 1176 was not affected as frequently or as severely because of its relatively flat-lying bathymetric character at the seaward edge of the slope basin. Gravity-driven slip probably was triggered by repeated uplift of the basin's southeastern margin during displacement along the two out-of-sequence thrusts that shape the basin's architecture (Fig. 10). Apparent dips of fanning reflectors within seismic unit A are generally toward the northwest. Axial planes of core-scale folds dip to the south and southwest (i.e., in the direction opposite to downslope movement). The chances of future occurrences of slope failure are minimal unless the basin's marginal relief experiences tectonic rejuvenation.

CONCLUSIONS

High rates of sedimentation within the Nankai Trough create favorable conditions for rapid frontal accretion. Shipboard data from Leg 190 of the Ocean Drilling Program show that the accretionary wedge has grown more than 40 km in width during the past 1 My. Numerous intraslope basins have formed above the Nankai accretionary prism. The sedimentary transition from slope-basin deposits to the underlying accreted turbidites cannot be defined precisely at Site 1175 or 1176 because their facies character changes gradually across the tectono-stratigraphic transition. Initial uplift of a frontal ridge evidently occurred in close proximity to the mouth of a submarine canyon. The seaward margin of the slope basin was sustained by fault-bend folding (ramp-to-flat transition) in the hanging wall of an out-of-sequence thrust. Because of this structural geometry, strata beneath the slope basin maintain low angles of dip and relatively mild degrees of deformation. The basin's overall stratigraphic succession thins and fines upward. We believe that sediment delivery paths to the slope basin were rerouted when subduction of the Kinan seamounts caused widespread damage across the Muroto forearc. Once the basin was isolated from its source of coarse siliciclastic sediment, turbidite sedimentation was replaced by hemipelagic settling. Uplift, landward tilting, and subhorizontal rotation of the seaward marginal ridge during the past 0.5 My triggered at least eight episodes of north- to northeast-directed mass wasting. The ridge has since been buried to its seaward sill point. Our opportunity to document this example of subduction-margin sedimentation has led to some important lessons for interpretation of inferred analogues in the rock record. Contacts, facies changes, and structural styles are not always as expected. Modern systems of this type are dynamic and unpredictable enough to warrant caution when applying generic conceptual models to interpretations of the rock record.

ACKNOWLEDGMENTS

We thank Captain Tom Ribbens, the crew, and technicians aboard JOIDES *Resolution* for their dedicated assistance during ODP Leg 190. This research used samples provided by the Ocean Drilling Program, sponsored by the U.S. National Science Foundation and participating countries under management of Joint Oceanographic Institutions, Inc. Thoughtful reviews by K. Pickering, R. Hiscott, and K. Marsaglia improved both the form and substance of the manuscript.

REFERENCES

Alexander, J., and Morris, S., 1994, Observations on experimental, nonchannelized, high-concentration turbidity currents and variations in deposits around obstacles: Journal of Sedimentary Research, v. A64, p. 899–909.

Ashi, J., and Taira, A., 1992, Structure of the Nankai accretionary prism as revealed from IZANAGI sidescan imagery and multichannel seismic reflection profiling: The Island Arc, v. 1, p. 104–115.

Bachman, S.B., 1982, The Coastal Belt of the Franciscan: youngest phase of northern California subduction, *in* Leggett, J.K., ed., Trench-Forearc Geology: Geological Society of London, Special Publication 10, p. 401–418.

Ballance, P.F., 1991, Gravity flows and rock recycling on the Tonga landward trench slope: relation to trench-slope tectonic processes: Journal of Geology, v. 99, p. 817–828.

Baltuck, M., von Huene, R., and Arnott, R.J., 1985, Sedimentology of the western continental slope of Central America, *in* von Huene, R., and Aubouin, J., eds., Initial Reports of the Deep Sea Drilling Project, v. 84: Washington, D.C., U.S. Government Printing Office, p. 921–937.

Blum, P., and Okamura, Y., 1992, Pre-Holocene sediment dispersal systems and effects of structural controls and Holocene sea-level rise from acoustic facies analysis; SW Japan forearc: Marine Geology, v. 108, p. 295–322.

Boyer, S.E., and Elliot, D., 1982, Thrust systems: American Association of Petroleum Geologists, Bulletin, v. 66, p. 1196–1230.

Brown, K.M., 1990, The nature and hydrologic significance of mud diapirs and diatremes for accretionary systems: Journal of Geophysical Research, v. 95, p. 8969–8982.

Chamot-Rooke, N., Renard, V., and Le Pichon, X., 1987, Magnetic anomalies in the Shikoku Basin: a new interpretation: Earth and Planetary Science Letters, v. 83, p. 214–228.

Coulbourn, W.T., 1986, Sedimentologic summary, Nankai Trough Sites 582 and 583, and Japan Trench Site 584, *in* Kagami, H., Karig, D.E., and Coulbourn, W.T., eds., Initial Reports of the Deep Sea Drilling Project, v. 87: Washington, D.C., U.S. Government Printing Office, p. 909–926.

Davey, F.J., Hampton, M., Childs, J., Fisher, M.A., Lewis, K., and Pettinga, J.R., 1986, Structure of a growing accretionary prism, Hikurangi margin, New Zealand: Geology, v. 14, p. 663–666.

Davis, E.E., and Hyndman, R.D., 1989, Accretion and recent deformation of sediments along the northern Cascadia subduction zone: Geological Society of America, Bulletin, v. 101, p. 1465–1480.

Dominguez, S., Malavielle, J., and Lallemand, S.E., 2000, Deformation of accretionary wedges in response to seamount subduction: Insights from sandbox experiments: Tectonics, v. 19, p. 182–196.

George, A.D., 1992, Deposition and deformation of an Early Cretaceous trench-slope basin deposit, Torlesse terrane, New Zealand: Geological Society of America, Bulletin, v. 104, p. 570–580.

Hampton, M.A., Lee, H.J., and Locat, J., 1996, Submarine landslides: Reviews of Geophysics, v. 34, p. 33–59.

Hibbard, J.P., Karig, D.E., and Taira, A., 1992, Anomalous structural evolution of the Shimanto accretionary prism at Murotomisaki, Shikoku Island, Japan: The Island Arc, v. 1, p. 133–147.

Jacobi, R.D., 1984, Modern submarine sediment slides and their implications for melange and the Dunnage Formation in north-central Newfoundland, *in* Raymond, L.A., ed., Melanges: Their Nature, Origin, and Significance: Geological Society of America, Special Paper 198, p. 81–102.

Kagami, H., and Mitusio, T., 1988, The Aki Canyon Fault—A boundary of the earthquake source area: Kochi University, Usa Marine Biological Institute, Reports, v. 10, p. 15–27.

Karig, D.E., and Angevine, C.L., 1986, Geologic constraints on subduction rates in the Nankai Trough, *in* Kagami, H., Karig, D.E., and Coulbourn, W.T., eds., Initial Reports of the Deep Sea Drilling Project, v. 87: Washington, D.C., U.S. Government Printing Office, p. 789–796.

Karig, D.E., Moore, G.F., Curray, J.R., and Lawrence, M.B., 1980, Morphology and shallow structure of the lower trench slope off Nias Island, Sunda arc, *in* Hayes, D.E., ed., The Tectonic and Geologic Evolution of Southeast Asian Seas and Islands: American Geophysical Union, Monograph 23, p. 179–208.

Kneller, B., Edwards, D., McCaffrey, W., and Moore, R., 1991, Oblique reflection of turbidity currents: Geology, v. 14, p. 250–252.

Kodaira, S., Takahashi, N., Park, J., Mochizuki, K., Shinohara, M., and Kimura, S., 2000, Western Nankai Trough seismogenic zone: Results from a wide-angle ocean bottom seismic survey: Journal of Geophysical Research, v. 105, p. 5887–5905.

Komar, P.D., 1970, The competence of turbidity current flow: Geological Society of America, Bulletin, v. 81, p. 1555–1562.

Kulm, L.D., von Huene, R., and the Shipboard Scientific Party, 1973, Initial Reports of the Deep Sea Drilling Project, v. 18: Washington, D.C., U.S. Government Printing Office, 1,077 p.

Lallemand, S., Culotta, R., and von Huene, R., 1989, Subduction of the Daiichi Kashima Seamount in the Japan Trench: Tectonophysics, v. 160, p. 231–247.

LE PICHON, X., IIYAMA, J.T., CHAMLEY, H., CHARVET, J., FAURE, M., FUJIMOTO, H., FURUTA, T., IDA, Y., KAGAMI, H., LALLEMANT, S., LEGGETT, J., MURUTA, A., OKADA, H., RANGIN, C., RENARD, V., TAIRA, A., AND TOKUYAMA, H., 1987a, Nankai trough and the fossil Shikoku Ridge: results of box 6 Kaiko survey: Earth and Planetary Science Letters, v. 83, p. 186–198.

LE PICHON, X., IIYAMA, T., CHAMLEY, H., CHARVET, J., FAURE, M., FUJIMOTO, H., FURUTA, T., IDA, Y., KAGAMI, H., LALLEMENT, S., LEGGETT, J., MURATA, A., OKADA, H., RANGIN, C., RENARD, V., TAIRA, A., AND TOKUYAMA, H., 1987b, The eastern and western ends of Nankai Trough: results of box 5 and box 7 Kaiko survey: Earth and Planetary Science Letters, v. 83, p. 199–213.

LEWIS, S.D., LADD, J.W., AND BRUNS, T.R., 1988, Structural development of an accretionary prism by thrust and strike-slip faulting: Shumagin region, Aleutian Trench: Geological Society of America, Bulletin, v. 100, p. 767–782.

MACKAY, M.E., MOORE, G.F., COCHRANE, G.R., MOORE, J.C., AND KULM, L.D., 1992, Landward vergence and oblique structural trends in the Oregon margin accretionary prism: implications and effect on fluid flow: Earth and Planetary Science Letters, v. 109, p. 477–491.

MARSAGLIA, K.M., INGERSOLL, R.V., AND PACKER, B., 1992, Tectonic evolution of the Japanese Islands as reflected in modal compositions of Cenozoic forearc and backarc sand and sandstone: Tectonics, v. 11, p. 1028–1043.

MARTINSEN, O., 1994, Mass movement, *in* Maltman, A., ed., The Geological Deformation of Sediments: London, Chapman & Hall, p. 127–165.

MIDDLETON, G.V., AND HAMPTON, M.A., 1976, Subaqueous sediment transport and deposition by sediment gravity flows, *in* Stanley, D.J., and Swift, D.J.P., eds., Marine Sediment Transport and Environmental Management: New York, John Wiley, p. 197–218.

MOORE, D.G., CURRAY, J.R., AND EMMEL, F.J., 1976, Large submarine slide (olistostrome) associated with Sunda Arc subduction zone, northeast Indian Ocean: Marine Geology, v. 21, p. 211–226.

MOORE, G.F., AND KARIG, D.E., 1976, Development of sedimentary basins on the lower trench slope: Geology, v. 4, p. 693–697.

MOORE, G.F., AND KARIG, D.E., 1980, Structural geology of Nias Island, Indonesia: implications for subduction zone tectonics: American Journal of Science, v. 280, p. 193–223.

MOORE, G.F., BILLMAN, H.G., HEHANUSSA, P.E., AND KARIG, D.E., 1980, Sedimentology and paleobathymetry of Neogene trench-slope deposits, Nias Island, Indonesia: Journal of Geology, v. 88, p. 161–180.

MOORE, G.F., KARIG, D.E., SHIPLEY, T.H., TAIRA, A., STOFFA, P.L., AND WOOD, W.T., 1991, Structural framework of the ODP Leg 131 area, Nankai Trough, *in* Taira, A., Hill, I.A., Firth, J.V., et al., Proceedings of the Ocean Drilling Program, Initial Reports, v. 131: College Station, Ocean Drilling Program, p. 15–20.

MOORE, G.F., TAIRA, A., BALDAUF, J., AND KLAUS, A., 2000, Deformation and fluid flow processes in the Nankai Trough accretionary prism: Ocean Drilling Program, Leg 190 Scientific Prospectus, online http://www-odp.tamu.edu/publications/prosp/190_prs/190toc.html.

MOORE, G.F., TAIRA, A., BANGS, N.L., KURAMOTO, S., SHIPLEY, T.H., ALEX, C.M., GULICK, S.S., HILLS, D.J., IKE, T., ITO, S., LESLIE, S.C., MCCUTCHEON, A.J., MOCHIZUKI, K., MORITA, S., NAKAMURA, Y., PARK, J.-O., TAYLOR, B.L., TOYAMA, G., YAGI, H., AND ZHAO, Z., 2001, Data Report: Structural setting of the Leg 190 Muroto Transect, *in* Moore, G.F., Taira, A., Klaus, A., et al., Proceedings of the Ocean Drilling Program, Initial Reports, v. 190: College Station, Texas (Ocean Drilling Program), online http://www-odp.tamu.edu/publications/190_IR/190ir.htm.

MOORE, J.C., AND KARIG, D.E., 1976, Sedimentology, structural geology, and tectonics of the Shikoku subduction zone, southwestern Japan: Geological Society of America, Bulletin, v. 87, p. 1259–1268.

MOORE, J.C., AND ALLWARDT, A., 1980, Progressive deformation of a Tertiary trench slope, Kodiak Islands, Alaska: Journal of Geophysical Research, v. 85, p. 4741–4756.

MOORE, J.C., WATKINS, J.S., SHIPLEY, T.H., MCMILLEN, K.J., BACHMAN, S.B., AND LUNDBERG, N., 1982, Geologic and tectonic evolution of a juvenile accretionary terrane along a truncated convergent margin: Synthesis of results from Leg 66 of the Deep Sea Drilling Project, southern Mexico: Geological Society of America Bulletin, v. 93, p. 847–861.

MORGAN, J.K., KARIG, D.E., AND MANIATTY, A., 1994, The estimation of diffuse strains in the toe of the western Nankai accretionary prism: A kinematic solution: Journal of Geophysical Research, v. 99, p. 7019–7032.

MOUNTNEY, N.P., AND WESTBROOK, G.K., 1996, Modeling sedimentation in ocean trenches: the Nankai Trough from 1 Ma to the present: Basin Research, v. 8, p. 85–101.

MUCK, M.M., AND UNDERWOOD, M.B., 1990, Upslope flow of turbidity currents: a comparison among field observations, theory, and laboratory models: Geology, v. 18, p. 54–57.

NAKAMURA, K., RENARD, V., ANGELIER, J., AZEMA, J., BOURGOIS, J., DEPLUS, C., FUJIOKA, K., HAMANO, Y., HUCHON, P., KINOSHITA, H., LABAUME, P., OGAWA, Y., SENO, T., TAKEUCHI, A., TANAHASHI, M., UCHIYAMA, A., AND VIGNERESSE, J.-L., 1987, Oblique and near collision subduction, Sagami and Suruga Troughs—preliminary results of the French–Japanese 1984 Kaiko cruise, Leg 2: Earth and Planetary Science Letters, v. 83, p. 229–242.

NIITSUMA N., 1989, Collision tectonics in the Southern Fossa Magna, Central Japan: Modern Geology, v. 14, p. 3–18.

OKINO, K., AND KATO, Y., 1995, Geomorphological study on a clastic accretionary prism: the Nankai Trough: The Island Arc, v. 4, p.182–198.

OKINO, K., SHIMAKAWA, Y., AND NAGAOKA, S., 1994, Evolution of the Shikoku Basin: Journal of Geomagnetics and Geoelectricity, v. 46, p. 463–479.

PANTIN, H.M., AND LEEDER, M.R., 1987, Reverse flow in turbidity currents: the role of internal solitons: Sedimentology, v. 34, p. 1143–1155.

PARK, J.-O., TSURU, T., KANEDA, Y., KONO, Y., KODAIRA, S., TAKAHASHI, N., AND KINOSHITA, H., 1999, A subducting seamount beneath the Nankai accretionary prism off Shikoku, southwest Japan: Geophysical Research Letters, v. 26, p. 931–934.

PICKERING, K.T., UNDERWOOD, M.B., AND TAIRA, A., 1992, Open-ocean to trench turbidity-current flow in the Nankai Trough: Flow collapse and reflection: Geology, v. 20, p. 1009–1102.

PICKERING, K.T., UNDERWOOD, M.B., AND TAIRA, A., 1993, Stratigraphic synthesis of the DSDP–ODP sites in the Shikoku Basin and Nankai Trough and accretionary prism, *in* Hill, I., Taira, A., Firth, J., and Vrolijk, P., eds., Proceedings of the Ocean Drilling Program, Scientific Results, v. 131: College Station, Ocean Drilling Program, p. 313–330.

PRATHER, B.E., BOOTH, J.R., STEFFENS, G.S., AND CRAIG, P.A., 1998, Classification, lithologic calibration, and stratigraphic succession of seismic facies of intraslope basins, deep-water Gulf of Mexico: American Association of Petroleum Geologists, Bulletin, v. 82, p. 701–728.

PRIOR, D.B., AND COLEMAN, J.M., 1984, Submarine slope instability, *in* Brunsden, D., and Prior, D.B., eds., Slope Instability: New York, John Wiley & Sons, p. 419–455.

SAMUEL, M.A., AND HARBURY, N.A., 1996, The Mentawai fault zone and deformation of the Sumatran forearc in the Nias area, *in* Hall, R., and Blundell, D., eds., Tectonic Evolution of Southeast Asia: Geological Society of London, Special Publication 106, p. 337–351.

SAMPLE, J.C., AND MOORE, J.C., 1987, Structural style and kinematics of an underplated slate belt, Kodiak and adjacent islands, Alaska: Geological Society of America, Bulletin, v. 99, p. 7–20.

SCHOLL, D.W., VON HUENE, R., VALLIER, T.L., AND HOWELL, D.G., 1980, Sedimentary masses and concepts about tectonic processes at underthrust ocean margins: Geology, v. 8, p. 564–568.

SENO, T., STEIN, S., AND GRIPP, A.E., 1993, A model for the motion of the Philippine Sea Plate consistent with NUVEL-1 and geological data: Journal of Geophysical Research, v. 98, p. 17,941–17,948.

SHIMAMURA, K., 1989, Topography and sedimentary facies of the Nankai Deep Sea Channel, *in* Taira, A., and Masuda, F., eds., Sedimentary Facies in the Active Plate Margin: Tokyo, Terra Scientific Publishing Company, p. 529–556.

SHIPBOARD SCIENTIFIC PARTY, 1975, Site 297, *in* Karig, D.E., Ingle, J.C., Jr., et al., Initial Reports of the Deep Sea Drilling Project, v. 31: Washington, D.C., U.S. Government Printing Office, p. 275–316.

SHIPBOARD SCIENTIFIC PARTY, 1991a, Site 808, *in* Taira, A., Hill, I., Firth, J.V., et al., Proceedings of Ocean Drilling Program, Initial Reports, v. 131: College Station, Texas, Ocean Drilling Program, p. 71–269.

SHIPBOARD SCIENTIFIC PARTY, 1991b, Explanatory notes, *in* Taira, A., Hill, I., Firth, J.V., et al., Proceedings of the Ocean Drilling Program, Initial Reports, v. 131: College Station, Texas, Ocean Drilling Program, p. 25–60.

SHIPBOARD SCIENTIFIC PARTY, 2001a, Site 1173, *in* Moore, G.F., Taira, A., Klaus, A., et al., Proceedings of the Ocean Drilling Program, Initial Reports, v. 190: College Station, Texas, Ocean Drilling Program, online http://www-odp.tamu.edu/publications/190_IR/190ir.htm.

SHIPBOARD SCIENTIFIC PARTY, 2001b, Site 1177, *in* Moore, G.F., Taira, A., Klaus, A., et al., Proceedings of the Ocean Drilling Program, Initial Reports, v. 190: College Station, Texas, Ocean Drilling Program, online http://www-odp.tamu.edu/publications/190_IR/190ir.htm.

SHIPBOARD SCIENTIFIC PARTY, 2001c, Site 1175, *in* Moore, G.F., Taira, A., Klaus, A., et al., Proceedings of the Ocean Drilling Program, Initial Reports, v. 190: College Station, Texas, Ocean Drilling Program, online http://www-odp.tamu.edu/publications/190_IR/190ir.htm.

SHIPBOARD SCIENTIFIC PARTY, 2001d, Site 1176, *in* Moore, G.F., Taira, A., Klaus, A., et al., Proceedings of the Ocean Drilling Program, Initial Reports, v. 190: College Station, Texas, Ocean Drilling Program, online http://www-odp.tamu.edu/publications/190_IR/190ir.htm.

SHIPBOARD SCIENTIFIC PARTY, 2001e, Leg 190 summary, *in* Moore, G.F., Taira, A., Klaus, A., et al., Proceedings of the Ocean Drilling Program, Initial Reports, v. 190: College Station, Texas, Ocean Drilling Program, online http://www-odp.tamu.edu/publications/190_IR/190ir.htm.

SINCLAIR, H.D., AND TOMASSO, M., 2002, Depositional evolution of confined turbidite basins: Journal of Sedimentary Research, v. 72, p. 451–456.

SMITH, G.W., HOWELL, D.G., AND INGERSOLL, R.V., 1979, Late Cretaceous trench-slope basins of central California: Geology, v. 7, p. 303–306.

SOH, W., PICKERING, K.T., TAIRA, A., AND TOKUYAMA, H., 1991, Basin evolution in the arc–arc Izu Collision Zone, Mio–Pliocene Miura Group, central Japan: Geological Society of London, Journal, v. 148, p. 317–330.

SOH, W., TANAKA, T., AND TAIRA, A., 1995, Geomorphology and sedimentary processes of a modern slope-type fan delta (Fujikawa fan delta), Suruga Trough, Japan: Sedimentary Geology, v. 98, p. 79–95.

STEVENS, S.H., AND MOORE, G.F., 1985, Deformational and sedimentary processes in trench slope basins of the western Sunda Arc, Indonesia: Marine Geology, v. 69, p. 93–112.

TAIRA, A., AND ASHI, J., 1993, Sedimentary facies evolution of the Nankai forearc and its implications for the growth of the Shimanto accretionary prism, *in* Hill, I.A., Taira. A., Firth, J.V., et al., Proceedings of the Ocean Drilling Program, Scientific Results, v. 131: College Station, Texas, Ocean Drilling Program, p. 331–341.

TAIRA, A., AND NIITSUMA, N., 1986, Turbidite sedimentation in the Nankai Trough as interpreted from magnetic fabric, grain size, and detrital modal analyses, *in* Kagami, H., Karig, D.E., and Coulbourn, W.T., eds., Initial Reports of the Deep Sea Drilling Project, v. 87: Washington, D.C., U.S. Government Printing Office, p. 611–632.

TAIRA, A., KATTO, J., TASHIRO, M., OKAMURA, M., AND KODAMA, K., 1988, The Shimanto Belt in Shikoku, Japan—evolution of Cretaceous to Miocene accretionary prism: Modern Geology, v. 12, p. 5–46.

TAIRA, A., HILL, I., FIRTH, J., BERNER, U., BRÜCKMANN, W., BYRNE, T., CHABERNAUD, T., FISHER, A., FOUCHER, J.-P., GAMO, T., GIESKES, J., HYNDMAN, R., KARIG, D., KASTNER, M., KATO, Y., LALLEMENT, S., LU, R., MALTMAN, A., MOORE, G., MORAN, K., OLAFFSON, G., OWENS, W., PICKERING, K., SIENA, F., TAYLOR, E., UNDERWOOD, M., WILKINSON, C., YAMANO, M., AND ZHANG, J., 1992, Sediment deformation and hydrogeology of the Nankai Trough accretionary prism: synthesis of shipboard results of ODP Leg 131: Earth and Planetary Science Letters, v. 109, p. 431–450.

TAYLOR, B., 1992, Rifting and the volcanic-tectonic evolution of the Izu–Bonin–Mariana Arc, *in* Taylor, B., Fujioka, K., et al., Proceedings of the Ocean Drilling Program, Scientific Results, v. 126: College Station, Texas, Ocean Drilling Program, p. 625–651.

UNDERWOOD, M.B., 1991, Submarine canyons, unconfined turbidity currents, and sedimentary bypassing of forearc regions: Critical Reviews in Aquatic Sciences, v. 4, p. 149–200.

UNDERWOOD, M.B., AND BACHMAN, S.B., 1982, Sedimentary facies associations within subduction complexes, *in* Leggett, J.K., ed., Trench-Forearc Geology: Geological Society of London, Special Publication 10, p. 537–550.

UNDERWOOD, M.B., AND KARIG, D.E., 1980, Role of submarine canyons in trench and trench-slope sedimentation: Geology, v. 8, p. 432–436.

UNDERWOOD, M.B., AND NORVILLE, C.R., 1986, Deposition of sand in a trench-slope basin by unconfined turbidity currents: Marine Geology, v. 71, p. 383–392.

UNDERWOOD, M.B., AND MOORE, G.F., 1995, Trenches and trench-slope basins, *in* Busby, C.J., and Ingersoll, R.V., eds., Tectonics of Sedimentary Basins: Cambridge, MA, Blackwell Science, p. 179–219.

UNDERWOOD, M.B., AND LAUGHLAND, M.M., 2001, Paleothermal structure of the Point San Luis slab of central California: Effects of Late Cretaceous underplating, out-of-sequence thrusting, and late Cenozoic dextral offset: Tectonics, v. 20, p. 97–111.

UNDERWOOD, M.B., ORR, R., PICKERING, K., AND TAIRA, A., 1993, Provenance and dispersal patterns of sediments in the turbidite wedge of Nankai Trough, *in* Hill, I.A., Taira, A., Firth, J.V., et al., Proceedings of the Ocean Drilling Program, Scientific Results, v. 131: College Station, Texas, Ocean Drilling Program, p. 15–34.

VAN DER LINGEN, G.J., AND PETTINGA, J.R., 1980, The Makara Basin: a Miocene slope-basin along the New Zealand sector of the Australian–Pacific obliquely convergent plate boundary, *in* Ballance, P.F., and Reading, H.G., eds., Sedimentation in Oblique-Slip Mobile Zones: International Association of Sedimentologists, Special Publication 4, p. 191–215.

VON HUENE, R., BOURGEOIS, J., MILLER, J., AND PAUTOT, G., 1989, A large tsunamogenic landslide and debris flow along the Peru Trench: Journal of Geophysical Research, v. 94, p. 1703–1714.

YAMAZAKI, T., AND OKAMURA, Y., 1989, Subducting seamounts and deformation of overriding forearc wedges around Japan: Tectonophysics, v. 160, p. 207–229.

Received 8 August 2001; accepted 20 September 2002.